

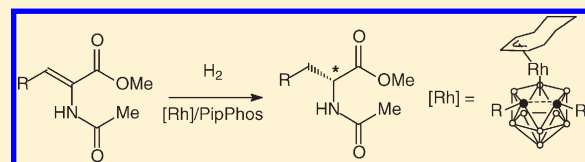
New Rhodacarborane–Phosphoramidite Catalyst System for Enantioselective Hydrogenation of Functionalized Olefins and Molecular Structure of the Chiral Catalyst Precursor [3,3-{(S)-PipPhos}₂-3-H-1,2-(*o*-xylylene)-*closo*-3,1,2-RhC₂B₉H₉]

Leonid S. Alekseev, Sergey E. Lyubimov, Fedor M. Dolgushin, Valentin V. Novikov, Vadim A. Davankov, and Igor T. Chizhevsky*

A. N. Nesmeyanov Institute of Organoelement Compounds of the RAS, 28 Vavilov Street, 119991 Moscow, Russian Federation

Supporting Information

ABSTRACT: Formally 16-electron *closo*- and *pseudocloso*-(η^3 -cyclooctenyl)rhodacarboranes of the general formula [3-{(1-3- η^3)-C₈H₁₃}-1,2-R,R'-3,1,2-RhC₂B₉H₉] (**1** (*closo*), R, R' = μ -1',2'-CH₂C₆H₄CH₂; **2** (*pseudocloso*), R = R' = PhCH₂) coupled in situ with the chiral phosphoramidite (S)-PipPhos (**3**) were found to catalyze an asymmetric hydrogenation of functionalized olefins (enamides) with enantioselectivities as high as 97–99.7% and with 92–100% conversions. The key catalyst precursor [3,3-{(S)-PipPhos}₂-3-H-1,2-(*o*-xylylene)-*closo*-3,1,2-RhC₂B₉H₉] (**16**), independently prepared by the stoichiometric reaction of **1** with **3** in benzene, was found to show of enantioselectivities and conversions upon the hydrogenation of prochiral enamides at the same levels as those observed for the relevant precursor formed in situ from **1** and **3**. The structure of **16** has been established on the basis of analytical and multinuclear NMR data as well as a single-crystal X-ray diffraction study. In contrast to complex **1**, complex **2** reacts with **3** to afford the unstable hydrido–rhodium species [3,3-{(S)-PipPhos}₂-3-H-1,2-(PhCH₂)₂-3,1,2-RhC₂B₉H₉] (**17**), the formation of which and further conversion into the salt [(S)-(PipPhos)₄Rh]⁺[7,8-(PhCH₂)₂-*nido*-7,8-C₂B₉H₁₀][−] (**18**) was detected by time-dependent ¹H NMR spectra. Some conclusions regarding the catalysis mechanistic pathway, which is consistent with that generally accepted for the rhodacarborane-catalyzed alkene hydrogenation, are made.



INTRODUCTION

Irida- and rhodacarboranes have been known since the mid-1970s,¹ and many of them have found applications as efficient catalyst precursors for homogeneous catalysis.² The first and most extensively studied catalyst precursors of this family are *closo*-bis(triphenylphosphine)hydridorhodacarborane, [H(PPh₃)₂-*closo*-3,1,2-RhC₂B₉H₁₁], and its 2,1,7- and 2,1,12-cage isomers.³ These icosahedral clusters usually display a unique tautomerism in solution between 18-electron Rh(III) *closo* and 16-electron Rh(I) *exo-nido* structures, the phenomenon first discovered by Hawthorne and co-workers in the early 1980s.⁴ The detailed studies of mechanistic aspects of metallocarborane catalysis have further revealed^{3d} that the catalytically active species of such systems contains a set of *exo*-B–Rh^{III}–H functions formed in solution by the reversible oxidative addition of Rh(I) to the terminal B–H bonds in the *exo-nido* precursor. These and other *exo-nido*-metallocarboranes turned out to be active and robust in a number of organic reactions such as the hydrogenation and isomerization of alkenes,^{3a–c,5} hydrogenolysis and hydrosilanolysis of alkenyl carboxylates,^{3d,e} cyclopropanation of alkenes with ethyl diazoacetate,⁶ Kharasch addition to alkenes,⁷ living polymerization of vinyl monomers,^{7a,8} and reduction of aromatic ketones to alcohols.⁹ On the other hand, there have been only very limited reports on either diastereo- and/or enantiocontrolled catalytic reactions employing transition-metal

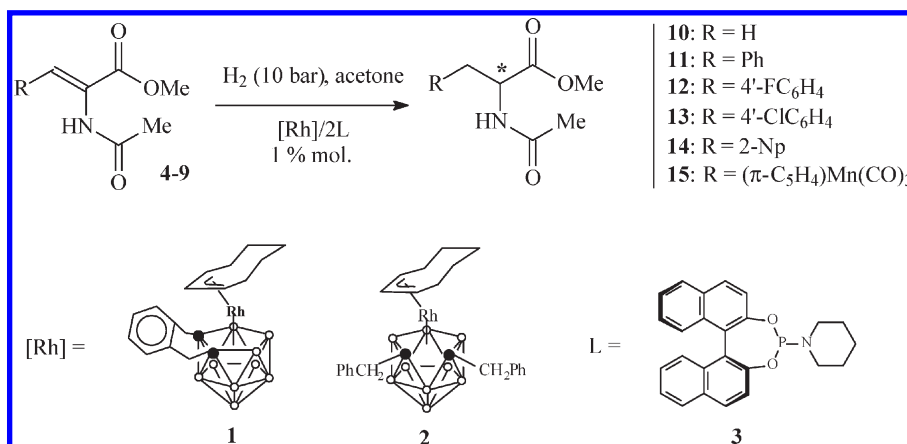
metallocarboranes of both *exo-nido* and *closo* structures,^{9,10} and among these only the (R)-BINAP-mediated catalyst of the formula [1,3- $\{\mu$ -(3- η^2 -(CH₂=CHCH₂CH₂))₂-3-H-3-PPh₃-*closo*-3,1,2-RhC₂B₉H₁₀] in ionic liquids has shown quite high enantioselectivity (>99%) in the hydrogenation of aromatic ketones to chiral alcohols under homogeneous catalysis by metallocarborane.⁹ In the present work, a novel rhodium-based catalytic system derived from the carbon-substituted *closo*- and *pseudocloso*-(η^3 -cyclooctenyl)rhodacarboranes of the general formula [3-{(1-3- η^3)-C₈H₁₃}-1,2-R, R'-3,1,2-RhC₂B₉H₉] (**1** (*closo*), R, R' = μ -1',2'-CH₂C₆H₄CH₂; **2** (*pseudocloso*), R = R' = PhCH₂) are described, which in combination with the chiral phosphoramidite (S)-PipPhos led to asymmetric hydrogenation of enamides with both excellent conversions and enantioselectivities.

RESULTS AND DISCUSSION

Using metalation reactions of the μ -chloride dimeric complexes [M(η^2 : η^2 -cyclooctadiene)Cl]₂ (M = Rh, Ir) with K⁺ salts of the isomeric *nido*-carborane monoanions [*nido*-7,*n*-R,R'-C₂B₉H₁₀][−] (*n* = 8, 9; R, R' = Alk, ArAlk), we have previously synthesized a series of *closo*- and *pseudocloso*-(η -carbocycle)metallocarborane

Received: December 27, 2010

Published: March 17, 2011

Scheme 1. Asymmetric Hydrogenation of Enamides 4–9 Catalyzed by (*S*)-PipPhos-Mediated Rhodacarborane SystemsTable 1. Asymmetric Hydrogenation Results for Enamides 4–9 Catalyzed by in Situ Generated Rhodacarborane/(*S*)-PipPhos Systems^a

entry	cat.	substrate	t, h	conversn, ^b %	ee, ^c %
1	1/2L	4	20	100	99.7 (R)
2	2/2L	4	20	100	99.5 (R)
3	1/2L	5	22	100	97 (R)
4	2/2L	5	18	100	91 (R)
5	1/2L	6	20	100	97 (R)
6	2/2L	6	20	100	98 (R)
7	1/2L	7	20	95	97 (R)
8	2/2L	7	20	100	96 (R)
9	1/2L	8	20	100	97 (R)
10	2/2L	8	20	96	97 (R)
11	1/2L	9	20	92	99.5 (R)
12	2/2L	9	20	100	99 (R)

^aAll reactions were performed in a cylindrical stainless steel reactor (20 mL capacity). Reaction conditions: 0.6 mmol of substrate, 0.006 mmol of **1** or **2**, 0.012 mmol of (*S*)-PipPhos, 5.0 mL of acetone at room temperature, 18–22 h. ^bConversions were determined by ¹H NMR spectroscopy. ^cEnantiomeric excesses were determined using HPLC (see the Supporting Information).

complexes of rhodium and iridium with either saturated 18-electron^{11,12} or formally unsaturated 16-electron^{11,13} metal centers. Among 16-electron complexes, there are several species with the exo-polyhedral (1–3- η^3)-cyclooctenyl-type ligands in which the electron deficiency is relieved either by an agostic C–H···M bonding interaction^{13a–c} or, as in the case of pseudocloso species,^{13d,e} via donation to a metal atom of an additional electron density released from the polyhedral C–C bond cleavage. Two rhodium complexes of both closo and pseudocloso types, **1**^{13c} and **2**,^{13e} are presented in this work, and each of them coupled in situ with the chiral phosphoramidite (*S*)-PipPhos (**3**),¹⁴ exhibiting in acetone solution excellent catalytic properties with regard to enantioselectivities and conversions upon the hydrogenation of prochiral enamides (Scheme 1). As summarized in Table 1, these unique phosphine-free catalytic systems give enantiomeric excesses of products **10–15** as high as 97–99.7%, which are among the highest

values observed for many other rhodium catalysts based upon BINOL-derived phosphoramidites.¹⁵ Very high to complete conversion for each of the tested substrates is achieved within 18–22 h. Clearly, the hydrogenation products thus obtained are valuable amino acid derivatives and therefore, if required, can easily be converted to the desired natural or unnatural amino acids without loss of optical purity.¹⁶

Hydrogenation reactions were carried out at ambient temperature in a cylindrical stainless steel reactor (20 mL capacity) charged with the catalyst precursor **1** or **2** and phosphoramidite **3**, taken in a 1/2 molar ratio, respectively, and the corresponding enamides **4–9** (catalyst/substrate = 1 mol/100 mol) in acetone solution (5 mL), followed by pressurization with argon (1.3 bar) and hydrogen gas (10 bar).

Preparation and Characterization of Hydrogenation Catalyst Precursors [3,3-((*S*)-PipPhos)₂-3-H-1,2- μ -(*o*-xylylene)-closo-3,1,2-RhC₂B₉H₉] (16**) and [3,3-((*S*)-PipPhos)₂-3-H-1,2- μ -(*o*-xylylene)-closo-3,1,2-RhC₂B₉H₉] (**17**) and the Catalytic Activity of **16**.** In an attempt to elucidate the nature of catalyst precursors used in situ for the hydrogenation of enamides **4–9**, a stoichiometric reaction of **1** with 2.2 equiv of (*S*)-PipPhos in benzene was independently studied and found to produce the air-stable hydrido–rhodium complex [3,3-((*S*)-PipPhos)₂-3-H-1,2- μ -(*o*-xylylene)-closo-3,1,2-RhC₂B₉H₉] (**16**) in 92% isolated yield. A single-crystal X-ray diffraction study (vide infra) combined with analytical and multinuclear multiple-resonance NMR data listed in the Experimental Section entirely confirmed the closo structure of **16** both in the solid state and in solution. The ¹H and ³¹P{¹H} NMR characteristics are particularly convincing. Thus, the ¹H NMR spectrum of **16** shows a somewhat broadened metal–hydride resonance at –8.15 ppm which is split into a triplet of doublets with the expected¹⁷ $J(^{31}\text{P}, ^1\text{H}) = 22.5$ Hz as well as $J(^{103}\text{Rh}, ^1\text{H})$ coupling of less than 5 Hz. The 242.97 MHz ³¹P{¹H} NMR spectrum of **16** contains a double set of AB quartets with the doublet components at 147.3 and 146.4 ppm (P_A , $J_{AB} = 55.0$, $J(^{103}\text{Rh}, \text{P}) = 208.0$ Hz) and 145.7 and 144.7 ppm (P_B , $J_{AB} = 55.1$, $J(^{103}\text{Rh}, \text{P}) = 220.8$ Hz) (Figure 1a). The correlation between doublets at 147.3 and 145.7 ppm as well as doublets at 146.4 and 144.7 ppm found in the 2D [³¹P–³¹P]-COSY spectrum (Figure 1b) further supports the assignment made for P_A and P_B components of the ABX spin system (X = ¹⁰³Rh) observed in the ³¹P{¹H} NMR spectrum of **16**.

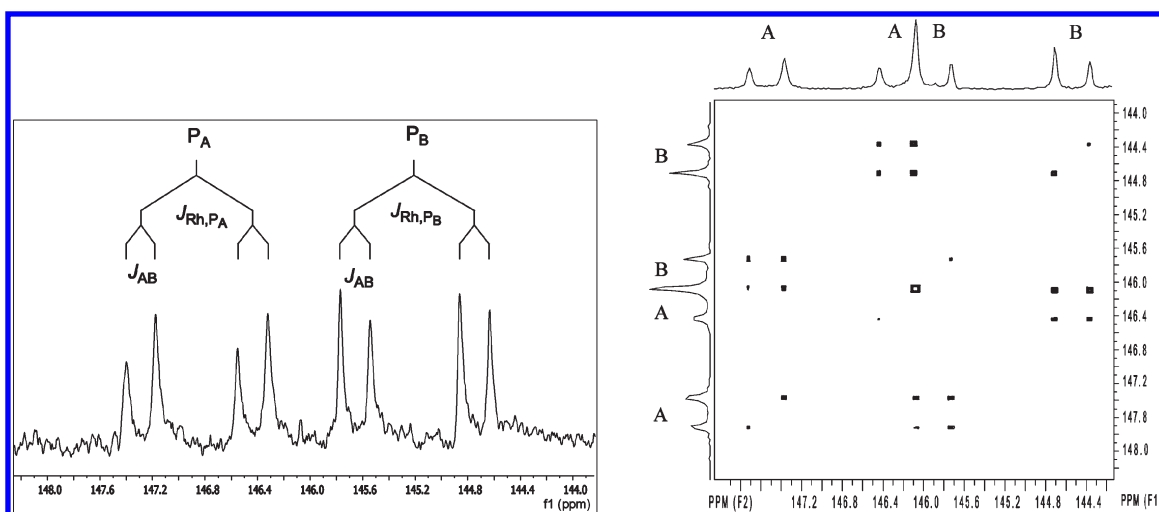


Figure 1. (a, left) 242.97 MHz $^{31}\text{P}\{^1\text{H}\}$ NMR spectrum for **16** in CD_2Cl_2 solution at 22 °C showing the assignment of the P_A and P_B resonances. (b, right) 161.97 MHz $[^{31}\text{P}\{^1\text{H}\}]-^{31}\text{P}\{^1\text{H}\}$ -COSY spectrum for **16** showing the assignments of the A and B parts of the spectrum (CD_2Cl_2 , 22 °C).

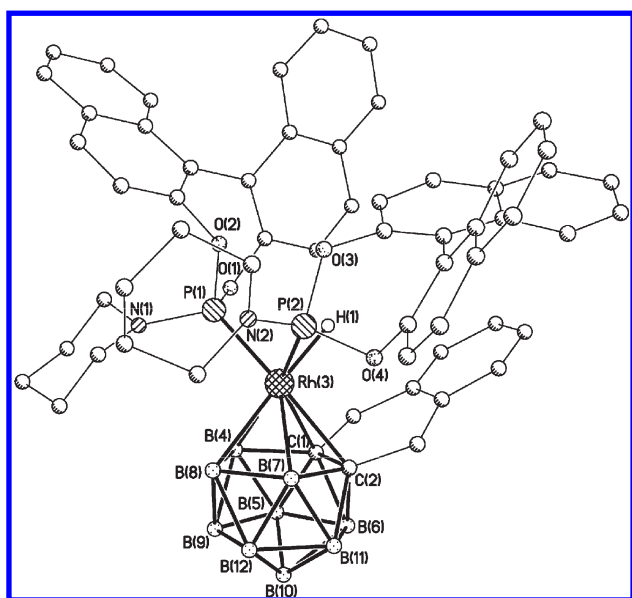


Figure 2. Molecular structure of $[3,3\text{-}\{(S)\text{-PipPhos}\}_2\text{-3-H-1,2-}(o\text{-xylylene})\text{-closo-3,1,2-RhC}_2\text{B}_9\text{H}_9]$ (**16**). All hydrogen atoms except H-(Rh) have been omitted for clarity. Selected interatomic distances (Å) and angles (deg) (values for both independent molecules are quoted): $\text{Rh}(3)\text{-P}(1) = 2.247(2), 2.242(3)$; $\text{Rh}(3)\text{-P}(2) = 2.259(2), 2.254(2)$; $\text{C}(1)\text{-C}(2) = 1.631(11), 1.560(13)$; $\text{Rh}(3)\text{-H}(1) = 1.69, 1.50$; $\text{Rh}(3)\text{-C}(1) = 2.324(9), 2.281(10)$; $\text{Rh}(3)\text{-C}(2) = 2.298(8), 2.277(9)$; $\text{Rh}(3)\text{-B}(4) = 2.254(9), 2.240(12)$; $\text{Rh}(3)\text{-B}(7) = 2.233(9), 2.235(10)$; $\text{Rh}(3)\text{-B}(8) = 2.290(8), 2.324(12)$; $\text{P}(1)\text{-Rh}(3)\text{-P}(2) = 94.39(8), 95.37(9)$; $\text{P}(1)\text{-Rh}(3)\text{-H}(1) = 76.2, 73.6$; $\text{P}(2)\text{-Rh}(3)\text{-H}(1) = 76.2, 59.3$.

An X-ray diffraction study on a crystal of complex **16** determined the structure shown in Figure 2. Two independent molecules have similar geometrical parameters (selected values for both are given in Figure 2). It has become apparent from the X-ray diffraction data that **16** in the crystalline phase represents a closo species containing an $(S)\text{-}(\text{PipPhos})_2\text{RhH}$ vertex with two phosphoramidites acting as monodentate ligands. Although icosahedral carborane-containing hydrido-rhodium complexes

Table 2. Asymmetric Hydrogenation of Enamides **4** and **5** Catalyzed by the Hydrido-Rhodium Complex **16** Independently Synthesized by the Reaction of **1** with **3**^a

entry	cat.	substrate	t, h	conversn, %	ee, %
1	16	4	18	100	99.4 (R)
2	16	5	18	100	98 (R)

^a Experimental conditions of catalytic reactions are the same as for the processes catalyzed by in situ generated $1/(S)\text{-PipPhos}$ systems (see Table 1).

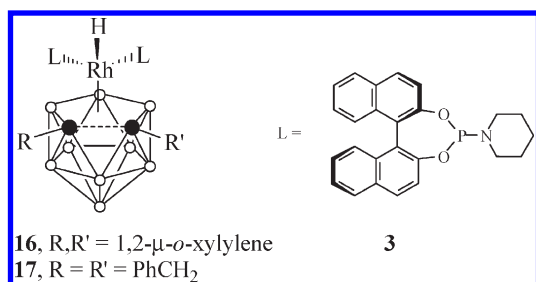
with different phosphorus-containing ligands at the metal vertex have been structurally characterized in numerous instances,^{4b,18} to the best of our knowledge, complex **16** is the first known closo-hydridometallacarborane incorporating chiral phosphoramidite-based ligands. Due to the presence of the bulky $\mu\text{-}(o\text{-xylylene})$ cage substituent, two phosphoramidite ligands and the rhodium-bound hydride in **16** adopt the sterically most favorable orientation with respect to the nido-carborane open face: both $(S)\text{-PipPhos}$ groups lie as far as possible from the cage substituent, while the terminal hydride, as the smallest ligand, is positioned over and bisects the cage C—C bond. The observed conformation of **16** agrees well with those predicted on the basis of the observed values of $J(\text{Rh},\text{P})$ and $J(\text{Rh},\text{H})$ coupling¹⁷ found from the aforementioned ^1H and $^{31}\text{P}\{^1\text{H}\}$ NMR spectra of **16**. The $o\text{-xylylene}$ substituent in **16** is displaced from the C_2B_3 plane of the cage ligand toward the metal atom in such a way that the angle between the normals to the cage pentagonal plane and the least-squares plane defined by the aromatic unit and bridging methylene carbons is 35°. This can be compared with similar angles found in $[3,3\text{-}(\text{Ph}_3\text{P})_2\text{-3-H-1,2-}\mu\text{-}(o\text{-xylylene})\text{-closo-3,1,2-RhC}_2\text{B}_9\text{H}_9]$ (38.7°)^{4a} and $[\text{exo-6,10-}\{(\text{Ph}_3\text{P})(\text{C}_6\text{H}_4\text{P})\text{Rh}\}\text{-6,10-}\mu\text{-}(\text{H})_2\text{-10-H-7,8-}\mu\text{-}(o\text{-xylylene})\text{-nido-7,8-C}_2\text{B}_9\text{H}_7]$ (81.0°);^{4a} bear in mind that one would expect the steric repulsion between the $o\text{-xylylene}$ group and the metal-containing moiety to be present in the former but not in the latter complex.

To test the ability of **16** to serve as a true catalyst precursor in the processes described above, asymmetric hydrogenation of enamides **4** and **5** catalyzed by complex **16** alone has been carried out. Remarkably, both reactions show the same levels of

enantioselectivities and conversions as observed for the precursor formed in situ from **1** and **3** under otherwise identical reaction conditions (Table 2). It is noteworthy that the hydrogenation process is strongly solvent dependent, and in chlorinated solvents such as CH_2Cl_2 no conversion was observed either for the independently prepared precursor **16** or for in situ generated adducts of **1** or **2** with phosphoramidite **3**.

Unlike complex **16**, which was shown to represent the observed closo isomer in all cases, i.e. both in solution (either in acetone or CH_2Cl_2) and in the solid state, the analogous hydrido–rhodium species $[\text{3,3-}\{(S)\text{-PipPhos}\}_2\text{-3-H-1,2-(PhCH}_2)_2\text{-3,1,2-RhC}_2\text{B}_9\text{H}_9]$ (**17**) (Chart 1) originating from **2** and **3** proved to be quite labile in solution due to a relatively fast

Chart 1. Schematic Representation of the Structurally Characterized (16**) and Proposed (**17**) Hydrido–Rhodium Complexes $[\text{3,3-}\{(S)\text{-PipPhos}\}_2\text{-3-H-1,2-R,R'-3,1,2-RhC}_2\text{B}_9\text{H}_9]$**



conversion into the new ionic species **18**. This latter complex could be prepared independently in 93% yield by treating **2** in C_6H_6 solution with a 4.5-fold molar excess of **3**. Elemental analysis for **18** as well as its ^1H and $^{31}\text{P}\{^1\text{H}\}$ NMR spectra (vide infra) are consistent with the formulation $[(S)\text{-}(\text{PipPhos})_4\text{-Rh}]^+[\text{7,8-(PhCH}_2)_2\text{-nido-7,8-C}_2\text{B}_9\text{H}_{10}]^-$. The $^{11}\text{B}/^{11}\text{B}\{^1\text{H}\}$ NMR spectra of **18** were, to a large extent, identical with those of the starting carborane monoanion from which both **2** and **18** were derived. It should also be noted that the ionic complex itself was not active in the catalytic hydrogenation of enamides **4** and **5** (these were used as test examples).

Relatively fast transformation of **17** into the ionic complex **18** in the presence of **3** prevented us from obtaining the hydrido–rhodium species **17** from a stoichiometric reaction of **2** with **3**. Hence, for detection and characterization of **17** the ^1H NMR monitoring of the reaction of **2** in both CD_2Cl_2 or d_6 -acetone with either immediate addition of 4.2 equiv of **3**/equiv of **2** or with increasing amounts of **3** varying from 0.5 to 4.0 equiv/equiv of **2** was used. The time-dependent ^1H NMR experiment (Figure 3) clearly demonstrated that **17** is the primary intermediate in the formation of ionic complex **18**. In fact, complex **17** is observed in the ^1H NMR spectrum with the high-field resonance at -8.14 ppm (td, $^2J(^{31}\text{P}, ^1\text{H}) = 25.3$ Hz, $^1J(^{103}\text{Rh}, ^1\text{H}) = 9.6$ Hz) even when the first 0.5 equiv of **3** had been added to 1.0 equiv of **2**. The terminal metal hydride resonance in the ^1H NMR spectra of **17** first appeared at -8.14 ppm and then slowly disappeared (all within ca. 45–50 min) to form instead a set of broad resonances in the terminal B–H (ca. -0.25 to $+0.5$ ppm) and B–H–B bridging region (-2.46 ppm) that can be

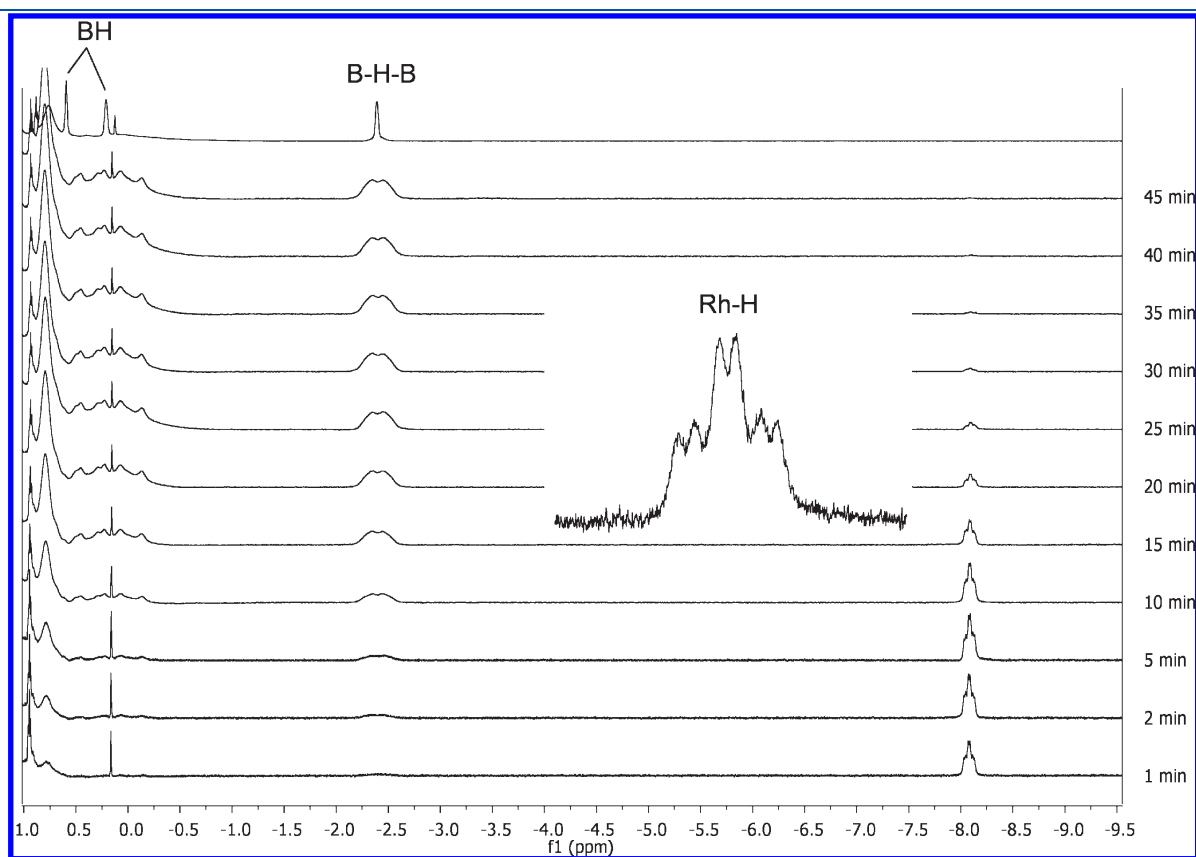


Figure 3. Series of ^1H NMR spectra from monitoring of the reaction of **2** with 4.2 equiv of **3** in CD_2Cl_2 with the upper $^1\text{H}\{^{11}\text{B}\}$ NMR spectrum of **18** (only the hydride region of the spectra is displayed).

attributed to the anionic cage of complex **18**; all these new resonances show an increase in intensity with a decrease in concentration of the hydrido–rhodium complex **17** (Figure 3) following the addition of each new portion of **3**. As expected, the resonances derived from the starting complex **2** in the ^1H NMR spectrum disappear completely after addition of 4.0 equiv of **3**.

The $^{31}\text{P}\{^1\text{H}\}$ NMR spectrum of **18** consists of 42 lines (Figure 4) and, therefore, is too complicated for an immediate

interpretation. Nevertheless, this spectrum has been successfully simulated as an $\text{AA}'\text{MM}'\text{X}$ spin system, where $\text{A}, \text{A}', \text{M}, \text{M}' = ^{31}\text{P}$, and $\text{X} = ^{103}\text{Rh}$. As shown in Figure 4, experimental and simulated spectra match very well, thus confirming the proposed formula of compound **18**.

The observed very large values of coupling constants between the nonequivalent phosphorus atoms ($^2J_{\text{AM}} = ^2J_{\text{A}'\text{M}'} = 506\text{ Hz}$) in **18** are indicative of phosphorus nuclei lying trans to each other.¹⁹ In contrast, the low values of other geminal couplings ($J_{\text{AA}'} = 45$

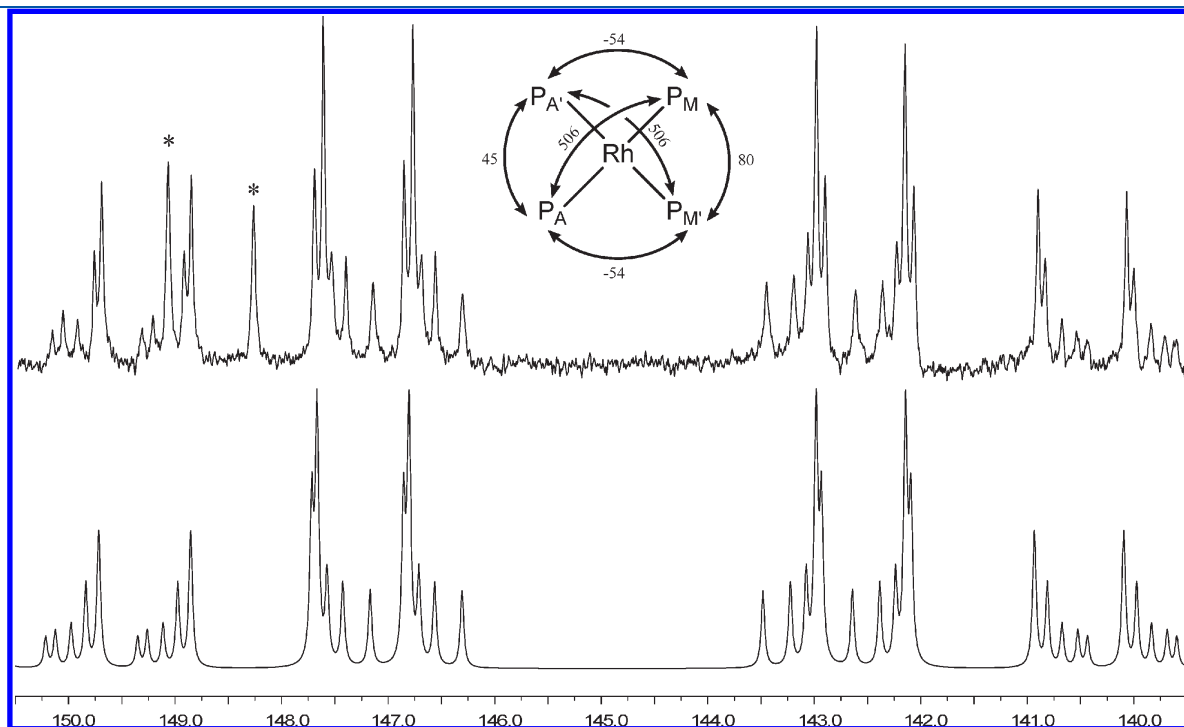
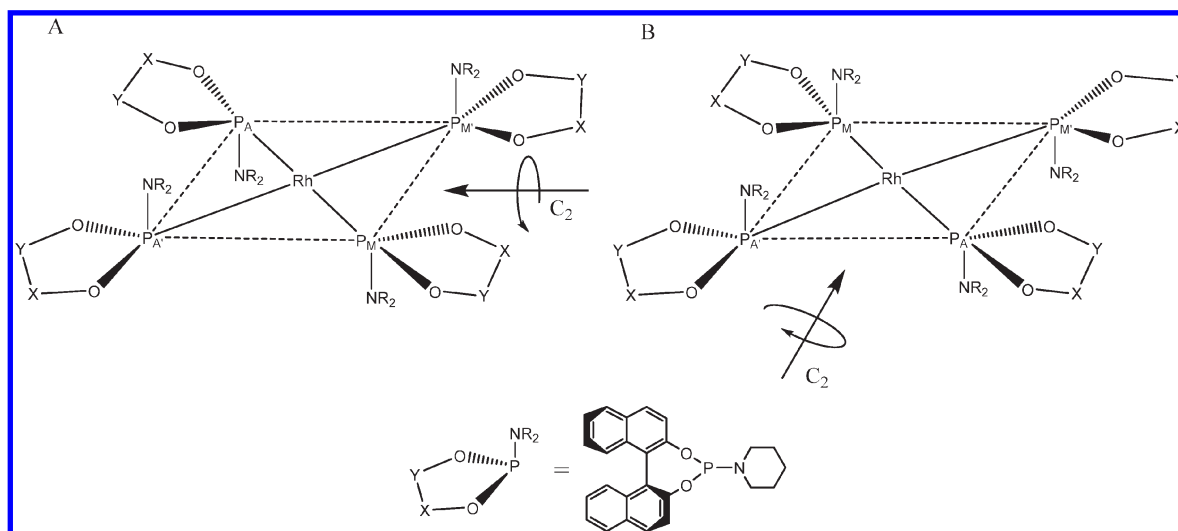


Figure 4. Experimental (above) and simulated (below) $^{31}\text{P}\{^1\text{H}\}$ NMR spectra (MestreNova 6.0.2 software) for an $\text{AA}'\text{MM}'\text{X}$ spin system with $\text{A}, \text{A}', \text{M}, \text{M}' = ^{31}\text{P}$, $\text{X} = ^{103}\text{Rh}$, $\delta(\text{A}) = \delta(\text{A}') = 141.70$, $\delta(\text{M}) = \delta(\text{M}') = 148.10\text{ ppm}$, $J_{\text{AA}'} = 45\text{ Hz}$, $J_{\text{AM}} = J_{\text{A}'\text{M}'} = 506\text{ Hz}$, $J_{\text{AM}'} = J_{\text{AM}} = -54\text{ Hz}$, $J_{\text{MM}'} = 80\text{ Hz}$, $J_{\text{AX}} = J_{\text{A}'\text{X}} = 184.5\text{ Hz}$, and $J_{\text{MX}} = J_{\text{M}'\text{X}} = 190\text{ Hz}$. Line widths for the phosphorus resonances are taken as 8 Hz. The resonance labeled with asterisks exhibited $J = 194.6\text{ Hz}$, which could be assigned to the $^{103}\text{Rh}-^{31}\text{P}$ coupling of (S)-PipPhos–rhodium species having a symmetrical structure.

Chart 2. Schematic Representation of Two Possible Structures (A and B) for Complex **18**



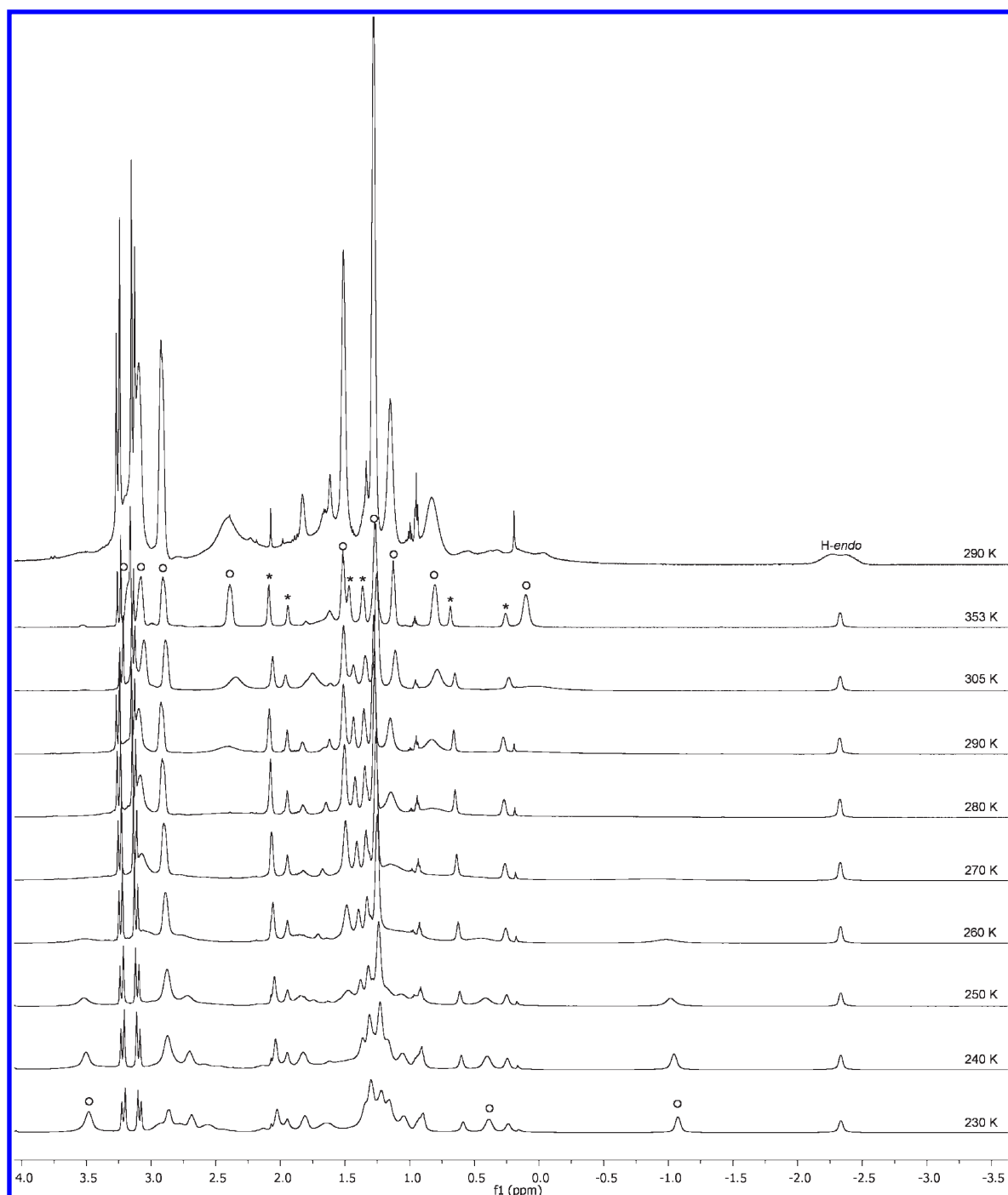


Figure 5. Variable-temperature $^1\text{H}\{^{11}\text{B}\}$ NMR spectra of complex **18**. The BH resonances of **18** are labeled with asterisks. The resonances of the piperidyl groups of **18** are labeled with circles. The upper nondecoupled ^1H NMR spectrum is given for comparison.

Hz, $J_{\text{AM}'} = J_{\text{A}'\text{M}} = -54$ Hz, $J_{\text{MM}'} = 80$ Hz) are typical of those for mutually cis P-atoms.^{19b} On the basis of these data and the square-planar geometry of the reported complex $[\text{Rh}(\text{MonoPhos})_4]\text{BF}_4$, which is the only structurally characterized rhodium species of this type with monodentate phosphoramidite based on BINOL,²⁰ we also suggest a square-planar (or slightly distorted) structure for compound **18** (Chart 2). The existence of two nonequivalent phosphorus groups in **18** can be accounted for by two possible structures (A and B) with the piperidine fragments located in both hemispheres; these two

structures, however, could not be differentiated on the basis of the NMR data alone.

Study of Dynamic Behavior of Ionic Complex 18 in Solution. There is one more feature in the NMR spectroscopic properties of **18** that is worthy of note. On the basis of literature data,^{4a} as well as the overcomplicated $^{31}\text{P}\{^1\text{H}\}$ NMR spectrum of **18** described above, it seemed logical to assume that a weak coordination between the carborane anion $[\text{7,8-(PhCH}_2)_2\text{-nido-7,8-C}_2\text{B}_9\text{H}_{10}]^-$ and the rhodium center of $[\{\text{(S)-PipPhos}\}_4\text{-Rh}]^+$ occurs through one or two B–H groups. Such a tight ion

pair might be fluxional in solution due to possible migration of the rhodium-containing moiety over the surface of the anionic carborane cage, by analogy with that observed in exo-nido species.^{4a}

Actually, the low-temperature (223 K) ¹H NMR spectrum of **18** at higher field displays a set of three resonances, one of which (at −2.46 ppm, as assigned above) originates from the bridging B···H···B hydrogen. Of the other two peaks at +0.30 and −1.18 ppm, at least the more shielded one or perhaps even both may possibly (in accord with the above assumption) be due to the terminal B–H hydrogens involved in a weak interionic B–H···Rh interaction. Since, however, all these and other cage B–H resonances in the boron-coupled ¹H NMR spectrum of **18** were broad and those in the region from −0.25 to +2.5 ppm partly overlapped, for their full assignment we have examined the low-temperature (223 K) boron-decoupled ¹H-¹¹B NMR spectrum (see Figure 5). Apart from a separate B–H–B resonance at −2.46 ppm, this spectrum displays a set of three 2H and three 1H peaks in the range from +0.25 to +2.2 ppm which, by comparison with those seen in the ¹H NMR spectrum, can correctly be assigned to the terminal B–H protons. Moreover, the ¹H-¹¹B NMR spectrum at 353 K appears to indicate the presence of another set of well-defined resonances integrated as having a total of 40 protons. These resonances, including those at +0.30 and −1.18 ppm, in the ¹H-¹¹B NMR spectrum at 230 K show no additional sharpening as compared with the boron-coupled ¹H NMR spectrum at the same temperature and were therefore assigned to the piperidine protons. A variable-temperature study showed it is precisely the piperidine peaks that exhibited dynamic behavior, while all B–H resonances in fact did not change their position in the spectra on passing from 223 to 353 K. Finally, in order to elucidate possible bonding interactions between [(S)-PipPhos]₄Rh⁺ and the carborane anion cage in **18**, an examination of its ¹H DOSY (diffusion ordered spectroscopy) spectrum was undertaken (see the Supporting Information). The presence of two independent sets of signals with different diffusion coefficients, corresponding to [(S)-PipPhos]₄Rh⁺ and the carborane anion cage, respectively, suggests the separate diffusion of these moieties in solution.

We, therefore, concluded that (i) no specific interaction exists between the cationic [(S)-PipPhos]₄Rh⁺ moiety and the carborane cage anion of compound **18** in solution, and the fluxional behavior of **18** revealed by the temperature-dependent ¹H NMR spectra can be attributed to the fluxionality of piperidyl substituents in its (S)-PipPhos ligands and (ii) presumably four (S)-PipPhos ligands in **18** produce a steric effect, which restricts the fluxionality of piperidyl substituents at low temperature (at least below 240 K), when they become “static”.

Some Conclusions Regarding the Hydrogenation Mechanistic Pathway. Assuming that the hydrogenation of enamides catalyzed by complexes **16** and **17** proceeds by a mechanism generally accepted for the rhodacarborane-catalyzed alkene hydrogenation and related reactions,^{3d} we attribute the catalytic activity observed to the presence of a unique equilibrium between 18 e Rh(III) closo and 16 e Rh(I) exo-nido rhodacarborane tautomers^{4a} wherein the key catalytically active species involves the exo-nido B–Rh^{III}–H array. This conclusion was based on the following observations. The intermediates formed in situ from the formally 16-electron clusters **1** and **2** and a chiral phosphoramidite **3** are, apparently, closo (or pseudocloso) rhodacarboranes containing a {(S)-(PipPhos)₂Rh^{III}H} vertex

in the metallacarborane frameworks of **16** and **17**, and complex **16** alone, as described above, is indeed highly active in the asymmetric hydrogenation of enamides. Evidently, the hydrogenation proceeds along a pathway that involves slow conversion of Rh(III) complexes **16** and **17** into the respective exo-nido Rh(I) tautomers in solution. However, no detectable amounts of these exo-nido tautomers in equilibrium either with **16** or **17** could be observed by NMR spectroscopy, perhaps owing to their high activity (and hence low concentration) with respect to oxidative addition reactions of [(R)-(PipPhos)₂Rh(I)] moiety with B–H cage vertices.

On the other hand, the formation of the ionic species **18** from the hydrido–rhodium species **17** provides some indirect evidence for the intermediate formation of the relevant exo-nido tautomer which, along with the competitive oxidative addition processes mentioned above, displaced the rhodium-containing moiety in the presence of a σ-donor (S)-PipPhos ligand^{4a,5b} to form [(S)-(PipPhos)₄Rh]⁺ stabilized by the [7,8-(PhCH₂)₂-nido-7,8-C₂B₉H₁₀][−] counterion.

CONCLUSIONS

The results of this study show that the use of a combination of the easily accessible chiral phosphoramidite **3** and 16-electron rhodacarboranes, either closo **1** or pseudocloso **2**, provides a potential route to new applications of such catalytically active metallacarborane systems for other enantioselective organic reactions as well as the opportunity to design new electronically deficient metallacarboranes previously untried as catalyst precursors in asymmetric organic reactions.

EXPERIMENTAL SECTION

General Considerations. All reactions were carried out under an argon atmosphere using standard Schlenk techniques. All solvents were distilled from appropriate drying agents prior to use. Compounds **1**,^{13c} **2**,^{13e} and **3**¹⁴ were prepared according to literature procedures. The ¹H, ¹H-¹¹B, ¹³C{¹H}, ³¹P{¹H}, and ¹¹B/¹¹B{¹H} NMR spectroscopic measurements, including VT NMR and 2D [¹H–¹H]-COSY and [¹H–¹³C]-HSQC spectra, were performed with a Bruker Avance-600 instrument using TMS as an internal reference or 85% H₃PO₄ and BF₃·Et₂O as external reference. Elemental analyses for **16** and **18** were performed by the Analytical Laboratory of the Institute of Organoelement Compounds of the Russian Academy of Sciences.

Preparation of [3,3-{(S)-PipPhos}₂-3-H-1,2-(*o*-xylylene)-closo-3,1,2-RhC₂B₉H₉] (16**).** Compounds **1** (30 mg, 0.067 mmol) and **3** (60 mg, 0.15 mmol) were dissolved in 1 mL of dry C₆H₆. After it was stirred for 1 h at ambient temperature, the color of the resulting mixture changed from red to a pale yellow; the reaction mixture was then diluted with 10 mL of *n*-hexane, and the precipitate that formed was separated by centrifugation. Washing with *n*-hexane (3 × 6 mL) and drying in vacuo afforded analytically pure **16** (70 mg, 92%). Anal. Calcd for C₆₀H₆₂B₉N₂O₄P₂Rh: C, 63.36; H, 5.49; N, 2.46; B, 8.56. Found: C, 63.32; H, 5.67; N, 2.42; B, 8.29. IR (KBr, cm^{−1}): 2541 (ν_{B–H}), 1942 (ν_{Rh–H}). ¹H NMR (600.22 MHz, CD₂Cl₂, 20 °C): δ 8.22–7.91 (total 6H, d-like each, CH_{aromatic}), 7.57–7.10 (total 18 H, m, CH_{aromatic}), 7.02 (t-like, 1H, C₆H₄), 6.95 (t-like, 1H, C₆H₄), 5.89 (d-like, 1H, C₆H₄), 5.75 (t-like, 1H, C₆H₄), 5.04 (d-like, 1H, CH_{aromatic}), 4.83 (d-like, 1H, CH_{aromatic}), 4.24 (dd-like, 1H, CH_AH_B, J_{H,H} = 17.4, J_{P,H} = 4.1 Hz), 3.87 (br d-like, 1H, CH_AH_B, J = 17.0 Hz), 3.56 (dd-like, 1H, CH_AH_B, J_{H,H} = 18.2, J_{P,H} = 5.3 Hz), 3.34 (br d-like, 4H, J = 29.0 Hz), 3.13 (br d-like, 4H, J = 29.0 Hz), 2.97 (dd-like, 1H, CH_AH_B, J_{H,H} = 18.0, J_{P,H} = 8.6 Hz), 1.62 (m, 2H, N(CH₂)₅), 1.53 (m, 2H, N(CH₂)₅), 1.42 (m, 4H,

$N(CH_2)_5$, 1.28 (m, 4H, $N(CH_2)_5$), -8.15 (t-like, 1H, $J_{P,H} = 22.5$ Hz). $^{11}B\{^1H\}$ NMR (128.38 MHz, CD_2Cl_2 , 20 °C): 0.0 (3B), -6.9 (2B), -9.0 (2B), -12.7 (2B). $^{13}C\{^1H\}$ NMR (150.93 MHz, CD_2Cl_2 , 20 °C): 149.8–120.5 (sets of doublet and singlet resonances, $C_{aromatic}$), 62.2, 61.9 (br q, C_{carb}), 45.1, 41.7 (CH_2), 47.5, 47.4, 27.1, 26.6, 25.79, 25.05, 24.66 (sets of doublets ($J_{C,P} = 4.0$ –5.5 Hz) and singlets, $N(CH_2)_5$). $^{31}P\{^1H\}$ NMR (242.97 MHz, CD_2Cl_2 , 20 °C): 146.75 (dd, $P_A, J_{AB} = 55.1, J_{P,Rh} = 208.0$ Hz), 145.32 (dd, $P_B, J_{AB} = 55.0, J_{P,Rh} = 220.8$ Hz). For the correlation 2D [1H – 1H]-COSY and [1H – ^{13}C]-HSQC spectra of **16** see the Supporting Information.

Preparation of the Ionic Complex [(S)-(PipPhos) $_4$ Rh] $^+$ [7,8-(PhCH $_2$) $_2$ -7,8-C $_2$ B $_9$ H $_{10}$] $^-$ (18**).** To a solution of **2** (60.0 mg, 0.11 mmol) in 5 mL of C_6H_6 was added **3** (200.0 mg, 0.50 mmol) as a solid, and the resulting reaction mixture was stirred overnight at room temperature. In the course of the reaction the color of the solution changed from orange to yellow, affording a yellow oil. Then *n*-hexane (10 mL) was added and an additional yellow powder precipitated from the mother liquor, while the oily deposits slowly solidified. The solids were isolated by centrifugation and dissolved in ca. 4 mL of CH_2Cl_2 , and the resulting solution was transferred to a flask containing 15 mL of *n*-hexane. The bulky precipitate that formed was again centrifuged, and the mother liquor was decanted. This procedure was repeated two times, and then the yellow powder was dried in vacuo to afford analytically pure **18** (212 mg, 92%). Anal. Calcd for $C_{116}H_{112}B_9N_4O_8P_4Rh$: C, 69.17; H, 5.60; N, 2.78; B, 4.83. Found: C, 69.18; H, 5.81; N, 2.66; B, 4.86. IR (KBr, cm^{-1}): 2519 (ν_{B-H}). $^1H\{^{11}B\}$ NMR (600.22 MHz, CD_2Cl_2 , 80 °C, $J = J(H,H)$, Hz): 8.36–6.99 (m, 54 H, $CH_{aromatic}$), 6.28 (d, 2H, $CH_{aromatic}$, $J = 8.7$), 5.73 (d, 2H, $CH_{aromatic}$, $J = 8.7$), 3.26 (d, 2H, $PhCH_2$, $J_{AB} = 15.3$), 3.16 (d, 2H, $PhCH_2$, $J_{AB} = 15.3$), 3.19, 3.09, 2.92, 2.40, 1.53, 1.28, 1.14, 0.82, 0.11 (set of 4H and 8H resonances (total 40 H), br m, $N(CH_2)_5$), 2.10 (br s, 2H, BH), 1.95 (br s, 1H, BH), 1.48 (br s, 2H, BH), 1.37 (br s, 2H, BH), 0.70 (br s, 1H, BH), 0.27 (br s, 1H, BH), -2.32 (br s, 1H, B–H–B). $^{11}B\{^1H\}/^{11}B$ NMR (128.38 MHz, CD_2Cl_2 , room temperature, $J = J(B,H)$, Hz): -9.4 (2B, $J = 137$), -10.7 (1B, $J = 168$), -17.5 (3B, $J = 125$), -18.3 (1B, $J = 127$), -33.8 (1B, $J = 129$), -36.5 (1B, $J = 141$). $^{13}C\{^1H\}$ NMR (150.93 MHz, CD_2Cl_2 , room temperature): 149.4–121.1 (sets of doublet and singlet resonances, $C_{aromatic}$), 61.8 (C_{carb}), 42.0 (CH_2Ph), 48.6, 26.9, 26.1, 24.9, 24.7 (sets of broad and sharp singlets, $N(CH_2)_5$). $^{31}P\{^1H\}$ NMR (242.97 MHz, CD_2Cl_2 , room temperature, all resonances are given as is): 150.2, 150.1, 149.9, 149.8, 149.7, 149.3, 149.2, 149.1*, 148.9, 148.8, 148.3*, 147.7, 147.6, 147.5, 147.4, 147.2, 146.9, 146.8, 146.7, 146.6, 146.3, 143.5, 143.2, 143.1, 143.0, 142.9, 142.6, 142.4, 142.3, 142.2, 142.1, 140.9, 140.8, 140.7, 140.6, 140.5, 140.1, 140.0, 139.9, 139.7, 139.6 (see Figure 4 caption for resonances labeled with asterisks).

X-ray Crystal Structure Analysis of Complex 16. Crystals of **16** ($C_{60}H_{62}B_9N_2O_4P_2Rh \cdot 2CH_2Cl_2 \cdot 0.25H_2O$, $M_r = 1311.61$) are monoclinic, space group $P2_1$, at 100 K: $a = 14.196(2)$ Å, $b = 16.434(2)$ Å, $c = 27.847(4)$ Å, $\beta = 94.117(3)^\circ$, $V = 6480(2)$ Å 3 , $Z = 4$, $d_{calcd} = 1.344$ g/cm 3 , $\mu = 0.526$ mm $^{-1}$. Data collection was carried out with a Bruker SMART APEX II diffractometer (λ (Mo K α) = 0.710 73 Å, ω scans, $2\theta < 56^\circ$) at 100 K. The structure was solved by direct methods and refined by the full-matrix least-squares technique against F^2 with anisotropic displacement parameters for all non-hydrogen atoms (disordered atoms of solvate molecules were refined in the isotropic approximation). The absolute configuration of **16** was determined by refinement of the Flack parameter ($x = -0.01(3)$). Hydrogen atoms of the hydride ligands and carborane cages were located from the Fourier synthesis; all other hydrogen atoms were placed geometrically and included in the structure factor calculations in the riding motion approximation. The refinement converged to $wR2 = 0.1280$ and $GOF = 1.058$ for 22 637 reflections ($R1 = 0.0548$ was calculated against F for 19 624 observed reflections with $I > 2\sigma(I)$). All calculations were performed using SHELXTL PLUS 5.0.²¹

■ ASSOCIATED CONTENT

S Supporting Information. Figures giving HPLC chromatograms of racemic samples and chiral hydrogenation products **10**–**15**, [1H – 1H]-COSY and [^{13}C – 1H]-HSQC NMR spectra of complexes **16** and **17**, DOSY 1H NMR spectrum of complex **17**, and [$^{31}P\{^1H\}$ – $^{31}P\{^1H\}$]-COSY spectrum of complex **16** and a CIF file giving X-ray crystallographic data for complex **16**. This material is available free of charge via the Internet at <http://pubs.acs.org>.

■ ACKNOWLEDGMENT

This work has been supported in part by Grants Nos. 09-0300211, 10-03-00837, and 10-0300505 from the Russian Foundation for Basic Research. We thank Dr. M. Esernizkaya for recording IR spectra and I. A. Godovikov for recording the [$^{31}P\{^1H\}$ – $^{31}P\{^1H\}$]-COSY NMR spectrum of complex **16**.

■ REFERENCES

- (1) See for instance: (a) Hoel, E. L.; Hawthorne, M. F. *J. Am. Chem. Soc.* **1973**, *95*, 2712. (b) Hoel, E. L.; Hawthorne, M. F. *J. Am. Chem. Soc.* **1975**, *97*, 6388. (c) Hardy, G. E.; Callahan, K. P.; Strouse, C. E.; Hawthorne, M. F. *Acta Crystallogr.* **1976**, *B32*, 264. (d) Jung, C. W.; Hawthorne, M. F. *Chem. Commun.* **1976**, 499. (e) Doi, J. A.; Teller, R. G.; Hawthorne, M. F. *Chem. Commun.* **1980**, 80.
- (2) For the reviews on catalyst design and catalysis by metallocarboranes see: (a) Hawthorne, M. F. In *Advances on Boron and the Boranes*; Liebman, J. F., Greenberg, R. E., Williams, R. E., Eds.; VCH: New York, 1988; Chapter 10, p 225. (b) Teixidor, F.; Nuñez, R.; Flores, M. A.; Demonceau, A.; Viñas, C. *J. Organomet. Chem.* **2000**, *614*–615, 48. (c) Grimes, R. *Coord. Chem. Rev.* **2000**, *200*–202, 773. (d) Teixidor, F.; Viñas, C.; Demonceau, A.; Nuñez, R. *Pure Appl. Chem.* **2003**, *75*, 1305. (e) Chizhevsky, I. T. *Coord. Chem. Rev.* **2007**, *251*, 1590. (f) Grishin, I. D.; Grishin, D. F. *Russ. Chem. Rev.* **2008**, *77*, 633.
- (3) (a) Paxson, T. E.; Hawthorne, M. F. *J. Am. Chem. Soc.* **1974**, *96*, 4674. (b) Behnken, P. E.; Belmont, J. A.; Busby, D. C.; Delaney, M. S.; King, R. E., III; Kreimendahl, C. W.; Marder, T. B.; Wilczynski, J. J.; Hawthorne, M. F. *J. Am. Chem. Soc.* **1984**, *106*, 3011. (c) Behnken, P. E.; Busby, D. C.; Delaney, M. S.; King, R. E., III; Kreimendahl, C. W.; Marder, T. B.; Wilczynski, J. J.; Hawthorne, M. F. *J. Am. Chem. Soc.* **1984**, *106*, 7444. (d) Belmont, J. A.; Soto, J.; King, R. E., III; Donaldson, A. J.; Hewes, J. D.; Hawthorne, M. F. *J. Am. Chem. Soc.* **1989**, *111*, 7475 and references therein. (e) Kang, H. C.; Hawthorne, M. F. *Organometallics* **1990**, *9*, 2327.
- (4) (a) Long, J. A.; Marder, T. B.; Behnken, P. E.; Hawthorne, M. F. *J. Am. Chem. Soc.* **1984**, *106*, 2979. (b) Knobler, C. B.; Marder, T. B.; Mizusawa, E. A.; Teller, R. G.; Long, J. A.; Behnken, P. E.; Hawthorne, M. F. *J. Am. Chem. Soc.* **1984**, *106*, 2990. (c) Long, J. A.; Marder, T. B.; Hawthorne, M. F. *J. Am. Chem. Soc.* **1984**, *106*, 3004. (d) Hewes, J. D.; Kreimendahl, C. W.; Marder, T. B.; Hawthorne, M. F. *J. Am. Chem. Soc.* **1984**, *106*, 5757.
- (5) (a) Teixidor, F.; Flores, M. A.; Viñas, C.; Kivekäs, R.; Sillanpää, R. *Angew. Chem., Int. Ed. Engl.* **1996**, *35*, 2251. (b) Viñas, C.; Flores, M. A.; Nuñez, R.; Teixidor, F.; Kivekäs, R.; Sillanpää, R. *Organometallics* **1998**, *17*, 2278. (c) Teixidor, F.; Flores, M. A.; Viñas, C.; Sillanpää, R.; Kivekäs, R. *J. Am. Chem. Soc.* **2000**, *122*, 1963.
- (6) (a) Demonceau, A.; Saive, E.; de Froidmont, Y.; Noels, A. F.; Hubert, A. J.; Chizhevsky, I. T.; Lobanova, I. A.; Bregadze, V. I. *Tetrahedron Lett.* **1992**, *33*, 2009. (b) Demonceau, A.; Simal, F.; Noels, A. F.; Viñas, C.; Nuñez, R.; Teixidor, F. *Tetrahedron Lett.* **1997**, *38*, 4079. (c) Demonceau, A.; Simal, F.; Noels, A. F.; Viñas, C.; Nuñez, R.; Teixidor, F. *Tetrahedron Lett.* **1997**, *38*, 7879. (d) Tutusaus, O.; Delfosse, S.; Demonceau, A.; Noels, A. F.; Nuñez, R.; Viñas, C.; Teixidor, F. *Tetrahedron Lett.* **2002**, *43*, 983.

- (7) (a) Simal, F.; Sebillé, S.; Demonceau, A.; Noels, A. F.; Nuñez, R.; Abad, M.; Teixidor, F.; Viñas, C. *Tetrahedron Lett.* **2000**, *41*, 5347. (b) Tutusaus, O.; Viñas, C.; Nuñez, R.; Teixidor, F.; Demonceau, A.; Delfosse, S.; Noels, A. F.; Mata, I.; Molins, E. *J. Am. Chem. Soc.* **2003**, *125*, 11830. (c) Tutusaus, O.; Delfosse, S.; Demonceau, A.; Noels, A. F.; Viñas, C.; Teixidor, F. *Tetrahedron Lett.* **2003**, *44*, 8421.
- (8) (a) Kolyakina, E. V.; Grishin, I. D.; Cheredilin, D. N.; Dolgushin, F. M.; Chizhevsky, I. T.; Grishin, D. F. *Russ. Chem. Bull.* **2006**, *55*, 89. (b) Grishin, I. D.; Kolyakina, E. V.; Cheredilin, D. N.; Chizhevsky, I. T.; Grishin, D. F. *Polym. Sci., Ser. A* **2007**, *49*, 1079. (c) Grishin, I. D.; Chizhevsky, I. T.; Grishin, D. F. *Dokl. Chem.* **2008**, *423*, 290. (d) Grishin, D. F.; Grishin, I. D.; Chizhevsky, I. T. In *Controlled/Living Radical Polymerization: Progress in ATRP*; Matyjaszewski, K., Ed.; American Chemical Society: Washington, DC, 2009; ACS Symposium Series 1023, Chapter 8, p 115.
- (9) Yinghuai, Z.; Carpenter, K.; Bun, C. C.; Bahnmüller, S.; Ke, C. P.; Srid, V. S.; Kee, L. W.; Hawthorne, M. F. *Angew. Chem., Int. Ed.* **2003**, *42*, 3792.
- (10) (a) Pirotte, B.; Felekidis, A.; Fontaine, M.; Demonceau, A.; Noels, A. F.; Delarge, J.; Chizhevsky, I. T.; Zinevich, T. V.; Pisareva, I. V.; Bregadze, V. I. *Tetrahedron Lett.* **1993**, *34*, 1471. (b) Felekidis, A.; Goblet-Stachow, M.; Liegeois, J. F.; Pirotte, B.; Delarge, J.; Demonceau, A.; Fontaine, M.; Noels, A. F.; Chizhevsky, I. T.; Zinevich, T. V.; Bregadze, V. I.; Dolgushin, F. M.; Yanovsky, A. I.; Struchkov, Yu. T. *J. Organomet. Chem.* **1997**, *536*, 405. (c) Brunner, H.; Apfelbacher, A.; Zabel, M. *Eur. J. Inorg. Chem.* **2001**, 917–934. (d) Brunner, H.; Rosenboem, S. *Monatsh. Chem.* **2000**, *131*, 1371.
- (11) Zinevich, T. V.; Safronov, A. V.; Vorontsov, E. V.; Petrovskii, P. V.; Chizhevsky, I. T. *Russ. Chem. Bull.* **2001**, *50*, 1702.
- (12) (a) Safronov, A. V.; Sokolova, M. N.; Vorontsov, E. V.; Petrovskii, P. V.; Barakovskaya, I. G.; Chizhevsky, I. T. *Russ. Chem. Bull.* **2004**, *53*, 1954. (b) Safronov, A. V.; Dolgushin, F. M.; Petrovskii, P. V.; Chizhevsky, I. T. *Organometallics* **2005**, *24*, 2964.
- (13) (a) Zinevich, T. V.; Safronov, A. V.; Dolgushin, F. M.; Tok, O. L.; Chizhevsky, I. T. *Russ. Chem. Bull.* **2001**, *50*, 2254. (b) Safronov, A. V.; Zinevich, T. V.; Dolgushin, F. M.; Vorontsov, E. V.; Tok, O. L.; Chizhevsky, I. T. *J. Organomet. Chem.* **2003**, *680*, 111. (c) Safronov, A. V.; Zinevich, T. V.; Dolgushin, F. M.; Tok, O. L.; Vorontsov, E. V.; Chizhevsky, I. T. *Organometallics* **2004**, *23*, 4970. (d) Alekseev, L. S.; Dolgushin, F. M.; Korlyukov, A. A.; Godovikov, I. A.; Vorontsov, E. V.; Chizhevsky, I. T. *Organometallics* **2007**, *26*, 3868. (e) Alekseev, L. S.; Dolgushin, F. M.; Korlyukov, A. A.; Godovikov, I. A.; Vorontsov, E. V.; Chizhevsky, I. T. *J. Organomet. Chem.* **2009**, *694*, 1727.
- (14) Mrcic, N.; Minnaard, A. J.; Feringa, B. L.; de Vries, J. G. *J. Am. Chem. Soc.* **2009**, *131*, 8358.
- (15) For selected examples: (a) Reetz, M. T.; Meiswinkel, A.; Mehler, G.; Angermund, K.; Graf, M.; Thiel, W.; Mynott, R.; Blackmond, D. G. *J. Am. Chem. Soc.* **2005**, *127*, 10305. (b) Reetz, M. T. *Angew. Chem., Int. Ed.* **2008**, *47*, 2556. (c) Teichert, J. F.; Feringa, B. L. *Angew. Chem., Int. Ed.* **2010**, *49*, 2486. (d) Bernsmann, H.; van den Berg, M.; Hoen, R.; Minnaard, A. J.; Mehler, G.; Reetz, M. T.; De Vries, J. G.; Feringa, B. L. *J. Org. Chem.* **2005**, *70*, 943.
- (16) (a) Boaz, N. W.; Large, S. E.; Ponasik, J. A.; Moore, M. K.; Barnette, T.; Nottingham, W. D. *Org. Process Res. Dev.* **2005**, *9*, 472. (b) Lyubimov, S. E.; Kuchurov, I. V.; Davankov, V. A.; Zlotin, S. G. *J. Supercrit. Fluids* **2009**, *50*, 118. (c) *Asymmetric Synthesis and Application of α -Amino Acids*; Soloshonok, V. A., Izawa, K., Eds.; American Chemical Society: Washington, DC, 2009.
- (17) Marder, T. B.; Baker, R. T.; Long, J. A.; Doi, J. A.; Hawthorne, M. F. *J. Am. Chem. Soc.* **1981**, *103*, 2988.
- (18) See for instance: (a) Delaney, M. S.; Knobler, C. B.; Hawthorne, M. F. *Inorg. Chem.* **1981**, *20*, 1341. (b) Delaney, M. S.; Teller, R. G.; Hawthorne, M. F. *Chem. Commun.* **1981**, 235. (c) Hewes, J. D.; Knobler, C. B.; Hawthorne, M. F. *Chem. Commun.* **1981**, 206. (d) Hewes, J. D.; Thompson, M.; Hawthorne, M. F. *Organometallics* **1985**, *4*, 13. (e) Chizhevsky, I. T.; Pisareva, I. V.; Petrovskii, P. V.; Bregadze, V. I.; Dolgushin, F. M.; Yanovsky, A. I.; Struchkov, Yu. T.; Hawthorne, M. F. *Inorg. Chem.* **1996**, *35*, 1386.
- (19) (a) Mann, B. E.; Masters, C.; Shaw, B. L. *J. Chem. Soc., Dalton Trans.* **1972**, 48. (b) Irvine, D. J.; Glidewell, C.; Cole-Hamilton, D. J.; Barnes, J. C.; Howie, A. *J. Chem. Soc., Dalton Trans.* **1991**, 1765.
- (20) Van den Berg, M.; Minnaard, A. J.; Haak, R. M.; Leeman, M.; Schudde, E. P.; Meetsma, A.; Feringa, B. L.; de Vries, A. H. M.; Maljaars, C. E. P.; Willans, C. E.; Hyett, D.; Boogers, J. A. F.; Henderickx, H. J. W.; de Vries, J. G. *Adv. Synth. Catal.* **2003**, *345*, 308.
- (21) Sheldrick, G. M. *Acta Crystallogr.* **2008**, *A64*, 112–122.